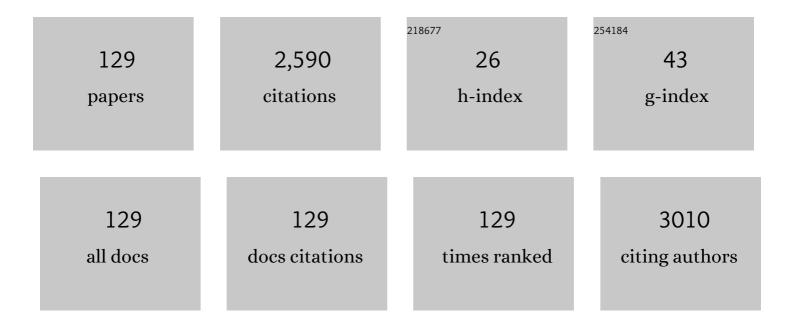
List of Publications by Year in descending order

Source: https://exaly.com/author-pdf/6468454/publications.pdf Version: 2024-02-01



GUANC-HULZHANC

#	Article	IF	CITATIONS
1	Sulfonated graphene as water-tolerant solid acid catalyst. Chemical Science, 2011, 2, 484-487.	7.4	247
2	Poly(amidoamine) modified graphene oxide as an efficient adsorbent for heavy metal ions. Polymer Chemistry, 2013, 4, 2164.	3.9	149
3	Characterization and adsorption mechanism of ZrO2 mesoporous fibers for health-hazardous fluoride removal. Journal of Hazardous Materials, 2018, 346, 82-92.	12.4	126
4	Synthesis of partially hydrogenated graphene and brominated graphene. Journal of Materials Chemistry, 2012, 22, 15021.	6.7	93
5	Electrospun SiO2-MgO hybrid fibers for heavy metal removal: Characterization and adsorption study of Pb(II) and Cu(II). Journal of Hazardous Materials, 2020, 381, 120974.	12.4	85
6	Photocatalytic selective hydroxylation of phenol to dihydroxybenzene by BiOI/TiO2 p-n heterojunction photocatalysts for enhanced photocatalytic activity. Applied Surface Science, 2018, 439, 1047-1056.	6.1	77
7	Growth, Morphology, Thermal, Spectral, Linear, and Nonlinear Optical Properties of <scp>l</scp> -Arginine Bis(trifluoroacetate) Crystal. Crystal Growth and Design, 2009, 9, 3251-3259.	3.0	65
8	Exfoliated MoS ₂ supported Au–Pd bimetallic nanoparticles with core–shell structures and superior peroxidase-like activities. RSC Advances, 2015, 5, 10352-10357.	3.6	53
9	High-temperature flexible, strength and hydrophobic YSZ/SiO2 nanofibrous membranes with excellent thermal insulation. Journal of the European Ceramic Society, 2021, 41, 1471-1480.	5.7	51
10	High temperature and high strength Y2Zr2O7 flexible fibrous membrane for efficient heat insulation and acoustic absorption. Chemical Engineering Journal, 2021, 416, 128994.	12.7	46
11	Lipase Immobilized on Graphene Oxide As Reusable Biocatalyst. Industrial & Engineering Chemistry Research, 2014, 53, 19878-19883.	3.7	44
12	Template-free synthesis of MgO mesoporous nanofibers with superior adsorption for fluoride and Congo red. Ceramics International, 2018, 44, 9454-9462.	4.8	42
13	Electrospinning fabrication of flexible Fe3O4 fibers by sol-gel method with high saturation magnetization for heavy metal adsorption. Materials and Design, 2020, 186, 108298.	7.0	42
14	Bulk growth and physical properties of diguanidinium phosphate monohydrate (G2HP) as a multi-functional crystal. CrystEngComm, 2014, 16, 930-938.	2.6	36
15	Rheological behavior, molecular structure of precursor and evolution mechanism: zirconia fibers from polyaceticzirconium precursors. Journal of Sol-Gel Science and Technology, 2015, 76, 482-491.	2.4	36
16	Improved preparation of electrospun MgO ceramic fibers with mesoporous structure and the adsorption properties for lead and cadmium. Ceramics International, 2019, 45, 3743-3753.	4.8	36
17	Ferrocene particles incorporated into Zr-based metal–organic frameworks for selective phenol hydroxylation to dihydroxybenzenes. RSC Advances, 2017, 7, 38691-38698.	3.6	34
18	Study on the third-order nonlinear optical properties of bis(tetrabutylammonium)bis(1,3-dithiole-2-thione-4,5-dithiolato)cadium. Optics Communications, 2005, 256, 256-260.	2.1	33

#	Article	IF	CITATIONS
19	Mesoporous ZrO 2 fibers with enhanced surface area and the application as recyclable absorbent. Applied Surface Science, 2017, 399, 288-297.	6.1	33
20	Controllable synthesis of Ag/AgCl@MIL-88A <i>via in situ</i> growth method for morphology-dependent photocatalytic performance. Journal of Materials Chemistry C, 2019, 7, 5451-5460.	5.5	33
21	The growth and properties of Ca3TaGa3Si2O14 single crystals. Journal of Crystal Growth, 2003, 253, 378-382.	1.5	31
22	Direct synthesis of phenol by novel [FeFe]-hydrogenase model complexes as catalysts of benzene hydroxylation with H2O2. RSC Advances, 2017, 7, 2934-2942.	3.6	30
23	Growth and properties of UV nonlinear optical crystal ZnCd(SCN)4. Materials Research Bulletin, 2001, 36, 1287-1299.	5.2	29
24	Electrospun mesoporous zirconia ceramic fibers for catalyst supporting applications. Ceramics International, 2018, 44, 282-289.	4.8	29
25	Violet light generation by frequency doubling of GaAlAs diode laser using a metallo-organic complex crystal ZnCd(SCN)4. Optics and Laser Technology, 2001, 33, 121-124.	4.6	26
26	Growth and characterization of a novel UV nonlinear optical crystal: [MnHg(SCN)4(H2O)2]·2C4H9NO. Journal of Crystal Growth, 2002, 234, 469-479.	1.5	26
27	A general strategy to prepare graphene-metal/metal oxide nanohybrids. Journal of Materials Chemistry, 2011, 21, 14498.	6.7	26
28	Crystal growth and physical properties of UV nonlinear optical crystal zinc cadmium thiocyanate, ZnCd(SCN)4. Chemical Physics Letters, 2001, 346, 393-406.	2.6	24
29	Crystal growth of high quality nonlinear optical crystals of l-arginine trifluoroacetate. Journal of Crystal Growth, 2007, 308, 130-132.	1.5	24
30	Blue-violet light second harmonic generation with CMTC crystals. Journal of Materials Science Letters, 2000, 19, 1255-1257.	0.5	23
31	Fabrication of zirconia mesoporous fibers by using polyorganozirconium compound as precursor. Microporous and Mesoporous Materials, 2009, 119, 230-236.	4.4	23
32	Modification of YSZ fiber composites by Al2TiO5 fibers for high thermal shock resistance. Journal of Advanced Ceramics, 2022, 11, 922-934.	17.4	23
33	Preparation and optical constants of the nano-crystal and polymer composite Bi4Ti3O12/PMMA thin films. Optics and Laser Technology, 2005, 37, 259-264.	4.6	22
34	Fabrication of La2Zr2O7 ceramic fibers via electrospinning method using different La2O3 precursors. Ceramics International, 2016, 42, 16633-16639.	4.8	22
35	Growth of zinc cadmium thiocyanate single crystal for laser diode frequency-doubling. Journal of Crystal Growth, 2001, 222, 755-759.	1.5	21
36	Crystal Growth and Characterization of a New Organometallic Nonlinear-Optical Crystal Material: MnHg(SCN)4(C3H8O2). Physica Status Solidi A, 2002, 191, 106-116.	1.7	21

GUANG-HUI ZHANG

#	Article	IF	CITATIONS
37	Third-order nonlinear optical properties inÂ[(C4H9)4N]2[Cu(C3S5)2]-doped PMMA thin film using Z-scan technique in picosecond pulse. Applied Physics A: Materials Science and Processing, 2010, 99, 279-284.	2.3	21
38	Measurement of l-arginine trifluoroacetate crystal nucleation kinetics. Journal of Crystal Growth, 2008, 310, 2590-2592.	1.5	20
39	Investigation of the nonlinear absorption and optical limiting properties of two [Q]2[Cu(C3S5)2] compounds. Optics and Laser Technology, 2010, 42, 732-736.	4.6	20
40	Electrospun fabrication, excellent high-temperature thermal insulation and alkali resistance performance of calcium zirconate fiber. Ceramics International, 2018, 44, 14013-14019.	4.8	20
41	Growth and properties of UV nonlinear optical crystal ZnCd(SCN)4. Materials Research Bulletin, 2003, 38, 1269-1280.	5.2	19
42	Flexible TiO2 ceramic fibers near-infrared reflective membrane fabricated by electrospinning. Ceramics International, 2019, 45, 6959-6965.	4.8	19
43	Water-stable metal–organic framework (UiO-66) supported on zirconia nanofibers membrane for the dynamic removal of tetracycline and arsenic from water. Applied Surface Science, 2022, 596, 153559.	6.1	19
44	Zirconia fiber membranes based on PVDF as high-safety separators for lithium-ion batteries using a papermaking method. Journal of Solid State Electrochemistry, 2019, 23, 269-276.	2.5	18
45	Lightweight and Resilient ZrO ₂ –TiO ₂ Fiber Sponges with Layered Structure for Thermal Insulation. Advanced Engineering Materials, 2022, 24, .	3.5	18
46	Preparation of a CeO2-nanoparticle thermal radiation shield coating on ZrO2 fibers via a hydrothermal method. Ceramics International, 2017, 43, 14183-14191.	4.8	17
47	Preparation, ferromagnetic and photocatalytic performance of NiO and hollow Co3O4 fibers through centrifugal-spinning technique. Materials Research Bulletin, 2016, 74, 319-324.	5.2	16
48	Effects of atmosphere and stabilizer on the decomposition and crystallization of polyacetylacetonatozirconium. Journal of Thermal Analysis and Calorimetry, 2017, 127, 1889-1895.	3.6	16
49	Study on nonlinear optical absorption properties of [(CH3)4N]2[Cu(dmit)2] by Z-scan technique. Optics and Laser Technology, 2009, 41, 209-212.	4.6	15
50	Water steam modified crystallization and microstructure of mesoporous TiO2 nanofibers. Ceramics International, 2018, 44, 2158-2164.	4.8	15
51	Preparation of mesoporous zirconia ceramic fibers modified by dual surfactants and their phosphate adsorption characteristics. Ceramics International, 2020, 46, 14019-14029.	4.8	15
52	Synthesis and characterization of Co2+: MgAl2O4 nanocrystal. Journal of Sol-Gel Science and Technology, 2006, 38, 245-249.	2.4	14
53	Biomimetic synthesis of interlaced mesh structures TiO2 nanofibers with enhanced photocatalytic activity. Journal of Alloys and Compounds, 2016, 668, 113-120.	5.5	14
54	High-temperature stable electrospun MgO nanofibers, formation mechanism and thermal properties. Ceramics International, 2017, 43, 16210-16216.	4.8	14

#	Article	IF	CITATIONS
55	Citric-acid-assisted sol-gel synthesis of mesoporous silicon-magnesium oxide ceramic fibers and their adsorption characteristics. Ceramics International, 2020, 46, 10105-10114.	4.8	14
56	Intracavity-frequency-doubling of a 946 nm Nd:YAG laser with cadmium mercury thiocyanate crystal. Optics and Laser Technology, 1998, 30, 291-293.	4.6	13
57	Studies on the conformational transformations of l-arginine molecule in aqueous solution with temperature changing by circular dichroism spectroscopy and optical rotations. Journal of Molecular Structure, 2012, 1026, 71-77.	3.6	13
58	Enhanced photocatalytic performance of Au/TiO2 nanofibers by precisely manipulating the dosage of uniform-sized Au nanoparticles. Applied Physics A: Materials Science and Processing, 2017, 123, 1.	2.3	13
59	Fabrication, heat-treatment and formation mechanism of MgO fiber using propionic acid as ligand. Ceramics International, 2017, 43, 2004-2011.	4.8	13
60	Hierarchically Microâ€/Nanostructured TiO ₂ /Micron Carbon Fibers Composites for Longâ€Life and Fastâ€Charging Lithiumâ€lon Batteries. ChemElectroChem, 2018, 5, 540-545.	3.4	13
61	Fabrication of dense and porous Li2ZrO3 nanofibers with electrospinning method. Applied Physics A: Materials Science and Processing, 2018, 124, 1.	2.3	13
62	Preparation, mechanical properties, and diffuse reflectance of YAG continuous fibers and nanofibers. Ceramics International, 2019, 45, 21213-21219.	4.8	13
63	Self-supporting super hydrophilic MgFe2O4 flexible fibers for Pb(II) adsorption. Separation and Purification Technology, 2021, 266, 118584.	7.9	13
64	Single crystal growth of MgB2 by using Mg-self-flux method at ambient pressure. Journal of Crystal Growth, 2004, 268, 123-127.	1.5	12
65	Crystallization process and microstructure of sol–gel derived Pb0.9La0.1Ti0.875O3 fine fibers with a novel heat-treatment process. Solid State Sciences, 2008, 10, 859-863.	3.2	12
66	Study on micro-crystallization, growth, optical properties and defects of a nonlinear optical crystal: MnHg(SCN)4. Journal of Crystal Growth, 2011, 317, 92-97.	1.5	12
67	Color tunable up-conversion emission from ZrO ₂ :Er ³⁺ ,Yb ³⁺ textile fibers. RSC Advances, 2016, 6, 103973-103980.	3.6	12
68	Polyaceticzirconium for zirconia continuous fibers: Polymeric evolution process and the relationship between polymeric structure and rheological behavior. Ceramics International, 2017, 43, 14176-14182.	4.8	12
69	The influence of phosphine ligand substituted [2Fe2S] model complexes as electro-catalyst on proton reduction. RSC Advances, 2018, 8, 42262-42268.	3.6	12
70	Crystal growth, structure and spectroscopic studies of a novel organic single crystal: Lâ€lysine pâ€nitrophenolate monohydrate (LLNP). Crystal Research and Technology, 2013, 48, 1087-1096.	1.3	11
71	Tubular structure TiO2/C/TiO2 hybrid derived from the waste of the fluff of chinar tree. Journal of Alloys and Compounds, 2018, 737, 774-789.	5.5	11
72	High-Efficient Photocatalytic Performance under Visible Light of Functionalized TiO ₂ Nanofibers via Steam and Pressure Co-Modification. Journal of Physical Chemistry C, 2019, 123, 17306-17317.	3.1	11

#	Article	IF	CITATIONS
73	Electrospun lanthanum-doped barium titanate ceramic fibers with excellent dielectric performance. Materials Characterization, 2021, 172, 110859.	4.4	11
74	Growth of cadmium mercury thiocyanate dimethylsulphoxide single crystal for laser frequency doubling. Progress in Crystal Growth and Characterization of Materials, 2000, 40, 75-79.	4.0	10
75	Edge dislocation and superstructure in MgB2superconducting crystals. Superconductor Science and Technology, 2005, 18, 1513-1516.	3.5	10
76	Atomic Force Microscopy Studies on {101} Surfaces of <scp> </scp> -arginine Trifluoroacetate Single Crystals. Journal of Physical Chemistry C, 2007, 111, 14165-14169.	3.1	10
77	Characterization and strong piezoelectric response of an organometallic nonlinear optical crystal: CdHg(SCN) ₄ (C ₂ H ₆ SO) ₂ . Journal of Materials Chemistry C, 2014, 2, 723-730.	5.5	10
78	Effects of cerium addition on the microstructure, mechanical properties and thermal conductivity of YSZ fibers. Ceramics International, 2018, 44, 7077-7083.	4.8	10
79	Zirconia/polyethylene terephthalate ceramic fiber paper separator for high-safety lithium-ion battery. Ionics, 2020, 26, 6057-6067.	2.4	10
80	Growth and Characterization of Series Nd:GdxLa1-xVO4 (x = 0.80, 0.60, 0.45) Crystals. Journal of Materials Research, 2002, 17, 556-562.	2.6	9
81	Formation of Barium Zirconate Fibers for Highâ€Temperature Thermal Insulation Applications. Journal of the American Ceramic Society, 2016, 99, 2913-2919.	3.8	9
82	Effects of pressure and atmosphere on the crystallization and grain refinement of zirconia fibers. Ceramics International, 2016, 42, 14189-14195.	4.8	9
83	Electrochemical catalysis investigation into the dynamic coordination properties of a pyridine-substituted [2Fe2S] model complex. International Journal of Hydrogen Energy, 2016, 41, 22991-22996.	7.1	9
84	Fabrication of dense barium zirconate fibers by electrospinning with different complex agents. Journal of the American Ceramic Society, 2017, 100, 4491-4499.	3.8	9
85	Large scale fabrication of magnesium oxide fibers for high temperature thermal structure applications. Ceramics International, 2017, 43, 1455-1459.	4.8	9
86	Electrospun flexible calcium zirconate fiber membrane with excellent thermal stability and alkali resistance. Ceramics International, 2022, 48, 12408-12414.	4.8	9
87	A novel organometallic nonlinear optical complex crystal: Cadmium mercury thiocyanate dimethyl-sulphoxide. Progress in Crystal Growth and Characterization of Materials, 2000, 40, 111-114.	4.0	8
88	Synthesis, crystal structure and saturable absorption in the near-IR regions of a new copper complex of dmit: hexadecyltrimethylammonium <i>bis</i> (2-thioxo-1,3-dithiole-4,5-dithiolato)-copper. Journal of Coordination Chemistry, 2008, 61, 768-775.	2.2	8
89	Titanium dioxide fibers prepared from two novel polytitanium precursors containing linear Ti–OH–Ti chains applied for photocatalytic degradation. Materials Letters, 2015, 153, 191-194.	2.6	8
90	Biomimetic synthesis of micro/nanostructured tubular TiO ₂ photocatalyst: adjusting the shape of the outer tube wall from nanoparticles to interlaced nanofibers and nanobelts. CrystEngComm, 2017, 19, 2312-2319.	2.6	8

GUANG-HUI ZHANG

#	Article	IF	CITATIONS
91	Preparation and fine thermal insulation performance of Gd2Zr2O7/ZrO2 composite fibers. Ceramics International, 2020, 46, 1615-1620.	4.8	8
92	Physicochemical properties and theoretical explanation of ZnCd(SCN)4 crystal. Materials Research Bulletin, 2004, 39, 1407-1416.	5.2	7
93	Nucleation growth mechanism and defects of nonlinear optical crystals of l-Arg·CF3COOH. Materials Letters, 2008, 62, 1986-1988.	2.6	7
94	Third-order nonlinearity and passive Q-switching of Cr^4+:YGG garnet crystal. Optics Letters, 2015, 40, 2421.	3.3	7
95	Synthesis, structural characterization, and chemical properties of pentacoordinate model complexes for the active site of [Fe]-hydrogenase. RSC Advances, 2016, 6, 84139-84148.	3.6	7
96	Strong Flexible Ceramic Nanofiber Membranes for Ultrafast Separation of Oil Pollutants. ACS Applied Nano Materials, 2022, 5, 9389-9400.	5.0	7
97	Preparation and transmission loss of the nano-crystal and polymer composite film BTO/PMMA. Optics and Laser Technology, 2003, 35, 291-294.	4.6	6
98	Effects of water vapor on the crystallization and microstructure manipulation of MgO ceramic fibers. Ceramics International, 2018, 44, 5257-5265.	4.8	6
99	Synthesis and characterization of a new lambda-type polymer for nonlinear optics based on carbazole derivative salt. Reactive and Functional Polymers, 2000, 46, 59-65.	4.1	5
100	Bis(tetraethylammonium) bis(2-thioxo-1,3-dithiole-4,5-dithiolato)cuprate(II). Acta Crystallographica Section E: Structure Reports Online, 2005, 61, m717-m719.	0.2	5
101	Distinct growth phenomenon observed on I-Arg·CF3COOH crystals. Current Applied Physics, 2009, 9, 22-25.	2.4	5
102	Seedless growth of ZnO nanorods on TiO ₂ fibers by chemical bath deposition. CrystEngComm, 2016, 18, 1215-1222.	2.6	5
103	Efficient removal of phosphate from aqueous solution by mesoporous Zr/La hydroxide fibers prepared with high-pressure steam heat treatment. Journal of Environmental Chemical Engineering, 2021, 9, 106697.	6.7	5
104	Study on the third-order nonlinear optical properties of bis(tetraethylammonium)bis(1,3-dithiole-2-thione-4,5-dithiolato)mercury. Journal of Optics, 2005, 7, 510-513.	1.5	4
105	Crystal growth, morphology, spectrographic characterization and thermal properties of 4,5â€bis(benzoylthio)â€1,3â€dithioleâ€2â€thione. Crystal Research and Technology, 2008, 43, 874-881.	1.3	4
106	Two novel polytitanium precursors containing linear Ti–(OH)2–Ti chains applied for the preparation of titanium dioxide fibers. Applied Physics A: Materials Science and Processing, 2015, 121, 723-730.	2.3	4
107	Bio-inspired Catalyst: [(μ -(SCH(CH2 CH3)CH2 S))Fe(CO)5]2 (μ,k1 ,k1 -DPPF) for Proton Reduction and Phenol Hydroxylation. ChemistrySelect, 2017, 2, 9407-9411.	1.5	4
108	Effects of the atmosphere on the high tensile strength and robust flexibility of Lu2O3 fibrous membrane. Ceramics International, 2021, 47, 8382-8388.	4.8	4

GUANG-HUI ZHANG

#	Article	IF	CITATIONS
109	Poly[bis(N-methylformamide)tetra-μ-thiocyanato-manganese(II)mercury(II)]. Acta Crystallographica Section C: Crystal Structure Communications, 2005, 61, m278-m280.	0.4	3
110	Bis(N-methylpyridinium) bis(2-thioxo-1,3-dithiole-4,5-dithiolato)zincate(II). Acta Crystallographica Section E: Structure Reports Online, 2005, 61, m2408-m2410.	0.2	3
111	Tetraphenylphosphonium bis(2-thioxo-1,3-dithiole-4,5-dithiolato)aurate(III) acetone solvate and ethyltriphenylphosphonium bis(2-thioxo-1,3-dithiole-4,5-dithiolato)aurate(III). Acta Crystallographica Section C: Crystal Structure Communications, 2008, 64, m46-m49.	0.4	3
112	Effect of the Terminal Ligands of [FeFe]â€Hydrogenase Model Complexes on Proton Reduction Properties and Catalytic Hydroxylation of Benzene. ChemistrySelect, 2017, 2, 3306-3310.	1.5	3
113	Effect of high-pressure vapor on the microstructure and mechanical properties of TiO2 continuous fibers. Ceramics International, 2022, 48, 10659-10666.	4.8	3
114	Preparation and Property for MgB ₂ Superconductive Phase Lines Using MgH ₂ and NaBH ₄ as Starting Materials by Laser Irradiation. Japanese Journal of Applied Physics, 2008, 47, 7857.	1.5	2
115	Nonlinear Optical Studies of [(C ₄ H ₉) ₄ N][Ni(dmit) ₂] by Z-Scan Technique. Chinese Physics Letters, 2011, 28, 107803.	3.3	2
116	ZnO long fibers: large scale fabrication, precursor and the transformation process, microstructure and catalytic performance. RSC Advances, 2014, 4, 57534-57540.	3.6	2
117	Guanidine-phosphate non-covalent interaction in LAP crystal growth solution evidenced from spectroscopy studies. Spectrochimica Acta - Part A: Molecular and Biomolecular Spectroscopy, 2015, 148, 12-17.	3.9	2
118	Effect of La2O3 on Grain Refinement and Thermal Conductivity of 6 mol % Y2O3–ZrO2 Fibers. Russian Journal of Inorganic Chemistry, 2019, 64, 1464-1468.	1.3	2
119	Hexadecyltrimethylammonium bis(2-thioxo-1,3-dithiole-4,5-dithiolato-κ2 S 4,S 5)nickelate(III). Acta Crystallographica Section E: Structure Reports Online, 2006, 62, m757-m759.	0.2	1
120	Butyltriphenylphosphonium bis(2-thioxo-1,3-dithiole-4,5-dithiolato)nickelate(III). Acta Crystallographica Section E: Structure Reports Online, 2006, 62, m1419-m1421.	0.2	1
121	STUDY ON THIRD-ORDER OPTICAL NONLINEARITY OF BIS(TETRABUTYLAMMONIUM)-Hg(dmit)2 BY FEMTOSECOND OPTICAL KERR GATE TECHNIQUE. Modern Physics Letters B, 2008, 22, 1573-1577.	1.9	1
122	INVESTIGATION OF THIRD-ORDER NONLINEAR OPTICAL PROPERTIES OF BFDT-DOPED PMMA THIN FILMS USING Z-SCAN TECHNIQUE. Modern Physics Letters B, 2009, 23, 3361-3368.	1.9	1
123	Magnetic dimer and tetramer based on dmit – Preparation, crystal structures, physicochemical characterization and magnetic properties. Inorganica Chimica Acta, 2013, 404, 68-76.	2.4	1
124	4,5-Bis(phenylsulfonylthio)-1,3-dithiolane-2-thione. Acta Crystallographica Section E: Structure Reports Online, 2005, 61, o1432-o1433.	0.2	0
125	Nonlinear optical studies of an organo-metallic complex by Z-scan technique. Proceedings of SPIE, 2007, , .	0.8	0
126	Preparation and transmission loss of the nano-crystal and polymer composite Bi 4 Ti 3 O 12 /PEK-c films. Proceedings of SPIE, 2008, , .	0.8	0

#	Article	IF	CITATIONS
127	Synthesis and electrochemical properties of [FeFe]-hydrogenase model complexes with acid-functionalized or base-functionalized ligands. Journal of Applied Electrochemistry, 2017, 47, 583-591.	2.9	Ο
128	Growth mechanism, dielectric, elastic and thermal properties of zinc cadmium thiocyanate crystal as a potential piezoelectric crystal. Chemical Physics Letters, 2017, 685, 401-409.	2.6	0
129	Preparation and excellent dielectric properties of flexible Ba0.7Sr0.29La0.01TiO3 composite fiber ceramics. Journal of Materials Science: Materials in Electronics, 2021, 32, 26359-26370.	2.2	Ο